Progress In Electromagnetics Research M, Vol. 101, 173–183, 2021

Compact Metal-Mountable UHF RFID Tag Antenna with Two Large C-Shaped Slots for On-the-Fly Tuning

Fwee-Leong Bong[1, *], Kunalen Thirappa[2], Eng-Hock Lim[2], and Kogulabalan Perumal[3]

Abstract—A compact folded-patch UHF RFID tag antenna (30 mm × 30 mm × 3 mm or $0.0912\lambda \times 0.0912\lambda \times 0.009\lambda$) is proposed for metallic surface applications. Two large C-shaped slots, which can be easily tuned by adjusting their lengths, are incorporated into the folded-patch for providing tuning mechanisms that can be employed in the production line for tuning the tag resonant frequency on the fly. The slots are tactfully embedded into the patch structure so that they occupy no footprint. The slots are large enough so that their lengths can be easily adjusted by employing a penknife and some copper tapes. This provides an impromptu tuning mechanism so that the tag resonant frequency can be easily corrected in the production line. With reference to the effective isotropic radiated power of 4 W, the proposed tag antenna can be read from 10 m on metal. The read range is found to be able to go beyond 5.5 m when the tag is placed on a dielectric with permittivity ranging from 1 to 12.

1. INTRODUCTION

The radio frequency identification (RFID) industry has been growing rapidly in the past decade owing to the advancement of semiconductor technology. In recent years, most of the UHF-band RFID tag antennas in the market are made of dipole [1] since it is simple in structure and easy to design. However, when a dipole is brought close to a metallic surface, its radiation efficiency can be greatly reduced due to the effect of the image currents [2]. Inserting an artificial-magnetic-conductor (AMC) for isolating the radiator from its ground layer [3] has been proposed to mitigate this problem. However, this can cause the tag profile to become higher. Some researchers have suggested the use of high-permittivity materials [4] for miniaturizing the tag size while preserving its performance. However, this method is not cost effective. To alleviate the issue mentioned above, the folded patch antennas [5], which can be easily fabricated by wrapping around a piece of soft dielectric foam substrate, have been proposed. These antennas are thin, simple to design, and low costs as they do not require extra shorting vias or walls which are usually fabricated by using the PCB processes. Usually, a tag antenna is required to have multiple tuning mechanisms for bringing down its resonance to the regulated UHF band [6]. Most of the tag antennas, however, are not able to provide impromptu tuning capabilities, as it is very difficult to change some of the small physical structures as soon as an antenna is made. This is very undesirable as a frequency-deviated tag can mean wastage in the production line. In practice, it is very common to have the tag resonance to deviate, and it always requires some impromptu tuning mechanisms which are large enough to be manipulated for tuning the tag resonant frequency back to the desired range.

In this paper, a novel folded-patch structure is proposed for designing a compact label tag that is mountable on metallic surface. Here, two large C-shaped slots are incorporated with the folded patch for providing impromptu tuning capability so that the tag can be easily tuned on-the-fly in the production

Received 1 January 2021, Accepted 1 March 2021, Scheduled 10 March 2021

* Corresponding author: Fwee-Leong Bong (bongfl@tarc.edu.my).

[1] Tunku Abdul Rahman University College, 77, Lorong Lembah Permai 3, Tanjung Bungah, Pulau Pinang 11200, Malaysia. [2] Universiti Tunku Abdul Rahman, Jalan Sungai Long, Bandar Sungai Long, Kajang, Selangor 43000, Malaysia. [3] OUM, Engineering Block C, Kelana Center Point, Jalan SS7/19, Kelana Jaya, Petaling Jaya, MY 4730q, Malaysia.

line. The two slots, whose lengths can be easily changed by employing copper tape and a cutter, are able to provide coarse and fine-tuning capabilities. It will be shown that combining the two slots makes the tag resonant frequency tunable effectively and arbitrarily to the desired resonant frequency once frequency deviation is found in the production. The two C-shaped slots are embedded into the patch structure, and it does not require additional footprint. Parametric analysis and measurements for real implementation scenarios have also been performed to understand the operation of the proposed tag antenna.

2. ANTENNA LAYOUT AND DESIGN PROCEDURE

Figure 1(a) shows the bare inlay (before folding) of the proposed tag antenna. It consists of a rectangular radiating patch and a ground patch that are formed by etching away the aluminum coating (9 µm) of a single-sided polyethylene terephthalate (PET) film (50 µm).

The two patches are wrapped symmetrically around a soft polyethylene foam (with $\varepsilon_r = 1.03$, $\tan\delta \sim 0.0001$) [7] with a dimension (30 mm × 30 mm and $h = 3$ mm) using adhesive. The foam acts as the structural support to shape the tag to its desired dimension and also isolates the radiating patch from the ground patch as shown in Fig. 1(b). The two patches are connected through a thin inductive stub located at the top-right corner of the radiating patch to guide the surface current to the ground, and it is able to provide sufficient inductive reactance for reducing the resonant frequency of the proposed tag. With reference to Fig. 1(a) and Fig. 1(b), it can be seen that a matching loop is

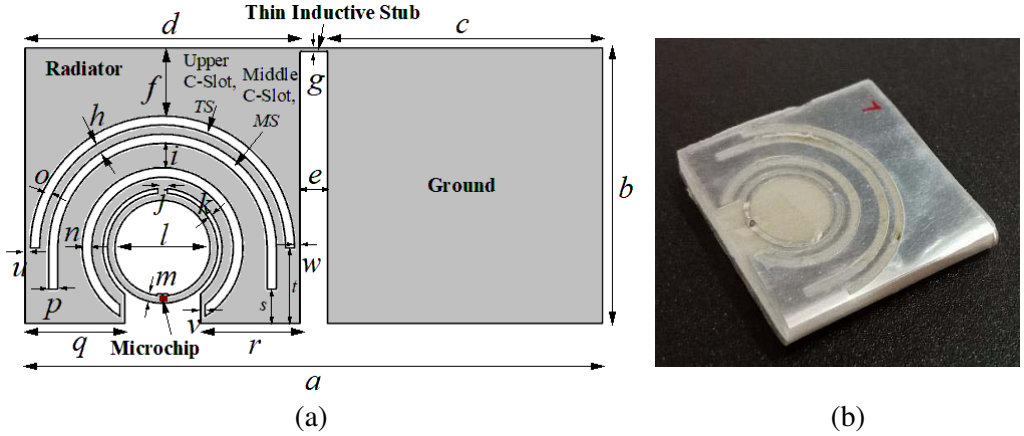

Figure 1. The proposed tag antenna geometry. (a) Bare inlay before folding. (b) Assembled tag antenna.

Table 1. The optimized design parameters of the proposed tag antenna.

Parameter	Dimension (mm)	Parameter	Dimension (mm)	Parameter	Dimension (mm)
a	63	j	1	s	3.68
b	30	k	0.5	t	8.15
c	29.95	l	10.4	u	0.55
d	29.95	m	0.8	v	0.5
e	3.1	n	1.05	w	0.51
f	7.35	o	1.05	MS	46.44
g	0.3	p	1.04	TS	43.74
h	0.95	q	10.86		
i	2.64	r	10.81		

tactfully embedded in the top patch of the tag. Different from the dipolar feeding structure in [8], the new tag here has tactfully embedded a matching loop and T-shaped matching stub into a folded-patch for achieving a very high degree of miniaturization, as can be seen in Fig. 1. The embedded matching loop, along with its associated T-shaped matching stub, is able to generate sufficiently high inductance for matching with the Impinj's Monza R6 [9] microchip impedance, which is highly capacitive. The chip input impedance (Z_c) is calculated to be $(11.9 - j118)\,\Omega$ at 922 MHz. The full-wave simulation of the proposed tag is done by using the CST Microwave Studio, and the optimized design parameters are given in Table 1.

To mimic the actual environment, for both the simulation and measurement, the proposed tag antenna is positioned at the center of a piece of 20 cm × 20 cm copper plate. The quality of impedance matching between the tag antenna and the microchip can be evaluated by the power transmission coefficient τ, which indicates the portion of power transferred to the antenna in actual. It is given by [10],

$$\tau = \frac{4R_cR_a}{|Z_c + Z_a|^2}, \quad 0 \le \tau \le 1 \tag{1}$$

where $Z_c = R_c + jX_c$ and $Z_a = R_a + jX_a$, which are the chip and antenna impedances, respectively. With reference to Fig. 2, good impedance matching is observed with $\tau \sim 1$ at the desired frequency of 922 MHz. To show the tuning capability of the thin inductive stub, the power transmission coefficient is simulated by introducing a minor change (Δg) to the stub width (g). As can be seen in Fig. 2,

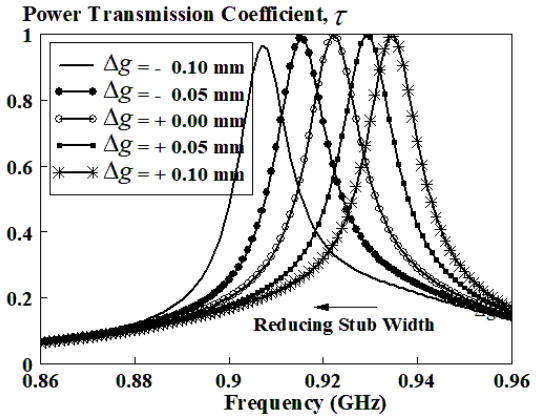

Figure 2. Simulated power transfer coefficient as a function of stub width g, being tested on a 20 cm × 20 cm backing metal plate.

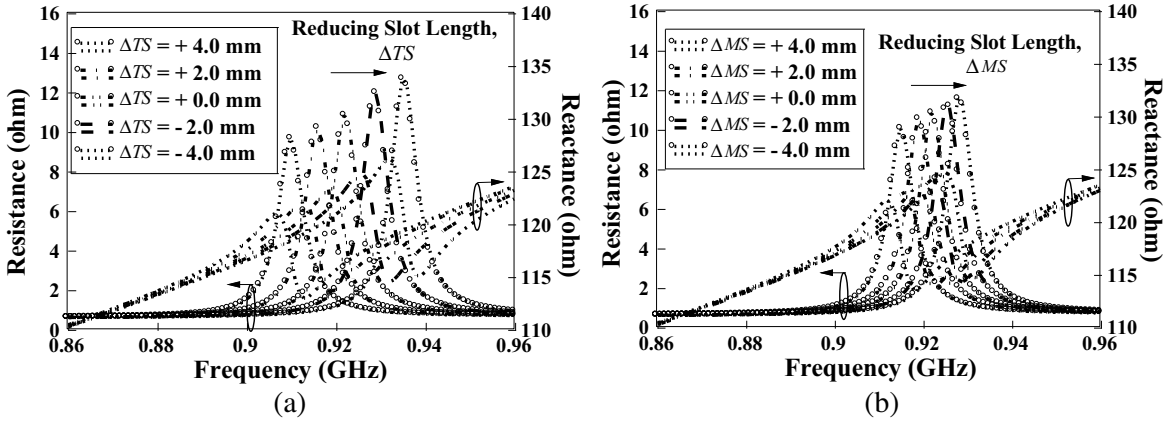

Figure 3. Effects of slot lengths on the tag impedance when the proposed tag is placed on a 20 cm × 20 cm backing metal plate. (a) Upper C-shaped slot, TS. (b) Middle C-shaped slot, MS.

changing the stub width is able to introduce a coarse tuning sensitivity of 14 MHz per 0.1 mm. It is good to mention that good impedance matching is maintainable by varying the width g. However, the inductive stub cannot be used for tuning the tag antenna on-the-fly in the production line as it is a small structure. It is very difficult to change the stub width once the inlay is etched.

To tackle this problem, two large C-shaped slots are introduced into the tag structure. With reference to Fig. 1(a), the upper C-shaped slot (named as TS) provides moderate tuning capability. It is tactfully etched on top of the radiating patch so that it does not require additional footprint. By decreasing ($-\Delta TS$) the slot length, with reference to Fig. 3(a), it is observed that the antenna's self-resonant frequency shifts higher with a rate of 3.25 MHz per 0.1 mm. Opposite trend is observed by increasing the slot length ($+\Delta TS$). On the other hand, as shown in Fig. 3(b), a finer tuning resolution can be achieved by the introduction of the middle C-shaped slot (named as MS). Reducing the slot length ($-\Delta MS$), again, causes the self-resonant frequency to move up with a rate of 0.2 MHz per 0.1 mm. In practice, the slots can be easily modified by a penknife and some copper tapes as they have a large dimension.

3. RESULTS AND DISCUSSION

The commercial UHF RFID testing system, Voyantic Tagformance [11], is used to conduct the measurements. The cable losses can be removed by the calibration. Read distance, tag sensitivity, and radiation pattern are the three main parameters to be measured here. The reference tag with known performance is first aligned in parallel with an 8 dBi linearly polarized reader antenna to achieve matching factor of 1 and calculate system path losses during system calibration. During tag performance measurement, the proposed tag antenna is located at the center of a metal plate (20 cm × 20 cm), which is attached to a Styrofoam block ($\varepsilon_r \approx 1$), as shown in Fig. 4. The same setting is also applied to the CST Microwave Studio full-wave simulation.

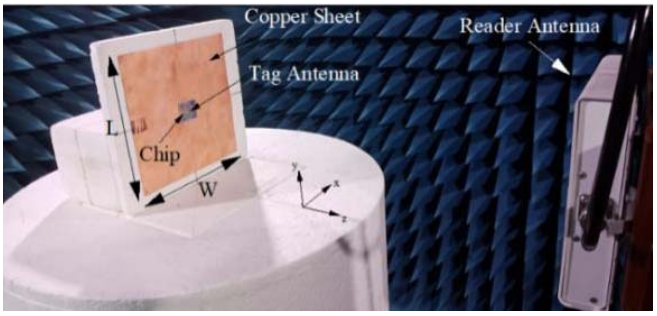

(a)

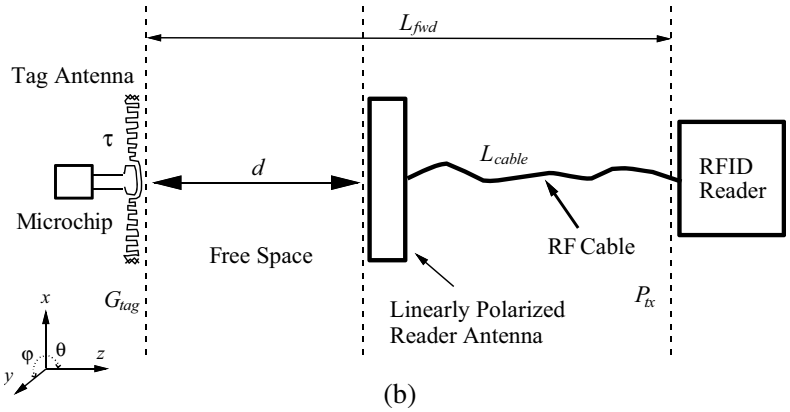

(b)

Figure 4. Commercial RFID Test system. (a) Tag measurement setup (on a 20 cm × 20 cm backing metal plate) in the anechoic chamber. (b) Schematic of the measurement setup in the anechoic chamber.

During the actual measurement process, the RFID reader transmits and changes its power gradually until a backscattered power is received from the tag. The threshold power P_{tx} is the minimum required reader's transmitted power to activate the tag, and with reference to P_{tx}, the tag turn-on power, usually called tag activation power or tag sensitivity P_{tag} [12, 13] can then be calculated as

$$P_{\text{tag}}\,[\text{dBm}] = P_{tx}\,[\text{dBm}] - |L_{\text{cable}}|\;[\text{dB}] + G_t\,[\text{dB}] - |\text{FSL}|\;[\text{dB}] = P_{tx}\,[\text{dBm}] - L_{fwd}\,[\text{dB}], \tag{2}$$

where $L_{fwd} = |L_{\text{cable}}|\,[\text{dB}] - G_t\,[\text{dB}] + |\text{FSL}|\,[\text{dB}]$ is the path loss attenuation. In the threshold measurement, the minimum power received by the microchip is the microchip's sensitivity, $P_{c,on}$, as stated in the datasheet [9].

$$P_{c,on}\,[\text{dBm}] = P_{\text{tag}}\,[\text{dBm}] + G_r\,[\text{dB}], \tag{3}$$

where G_r is the realized gain of the tag antenna. Moreover, the tag antenna gain can be expressed in linear scale as

$$G_r = \frac{P_{c,on}}{P_{\text{tag}}} \tag{4}$$

With reference to the maximum regulated radiated power P_{EIRP}, where $P_{\text{EIRP}} = P_t G_t$ and the tag's sensitivity P_{tag} which is measured by the reader, the theoretical achievable read distance $R_{\max}$ can then be obtained by [11],

$$R_{\max} = \frac{\lambda}{4\pi}\left[\frac{P_t G_t G_r}{P_{c,on}}\right]^{0.5} = \frac{\lambda}{4\pi}\left[\frac{P_{\text{EIRP}}}{P_{\text{tag}}}\right]^{0.5} \tag{5}$$

Figure 5 compares the measured and simulated realized gains. The measured realized gain is ~ -4 dB, and the tag resonant frequency is located at 912 MHz. The simulated tag resonance is observed to be 922 MHz with a gain level of approximately 2 dB higher than its measurement counterpart. With reference to Fig. 5, it can be seen that the optimum point of the measured tag sensitivity, which has the minimum power, is actually collocated with the maximum point of the measured realized gain, both of which are at 912 MHz. The discrepancy between the simulated (922 MHz) and measured (912 MHz) tag resonant frequencies is actually very small (1.08%), and it can be caused by experimental, fabrication, and component tolerances as an active device tends to have a larger manufacturing tolerance. It was a fair comparison as both of the simulation and measurement are done by including the same 20 cm × 20 cm metal plate. All measurements were conducted inside an anechoic chamber for obtaining the best results under a controlled environment. The measured tag sensitivity reaches its peak at -16 dBm at the resonance.

The simulated surface current distribution is shown in Fig. 6(a) at the resonant frequency of 922 MHz. Surface currents are observed to flow along the perimeters of the two slots, reflecting good resonant frequency tuning parameters. The currents are forced to flow in the direction of the inductive

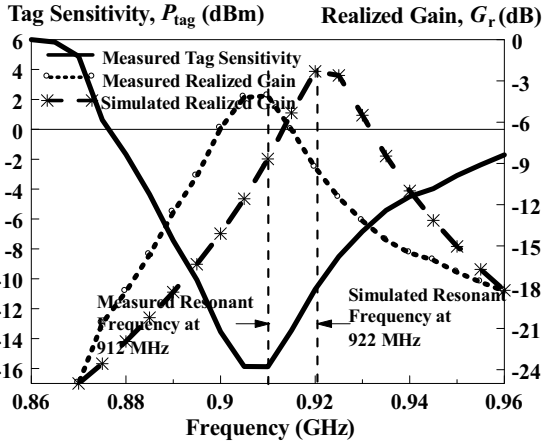

Figure 5. Measured and simulated realized gain G_r and the corresponding tag sensitivity P_{tag} in the direction of $\theta = 45°$ and $\emptyset = 0°$.

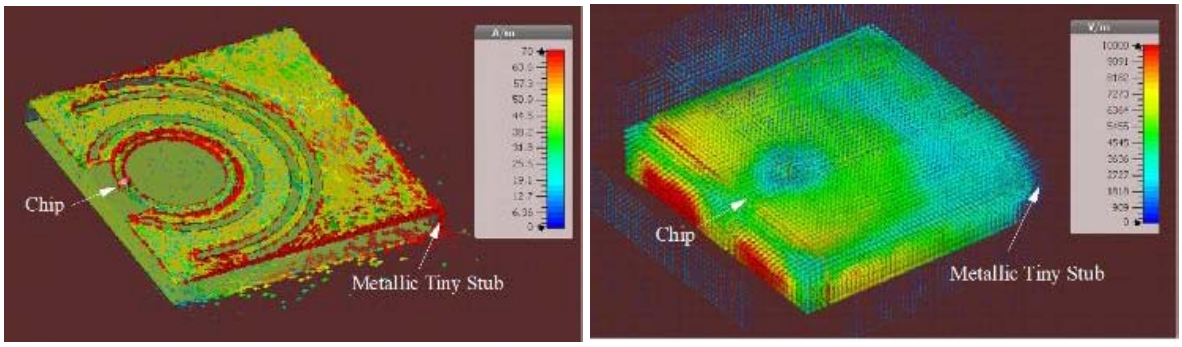

(a) (b)

Figure 6. Simulated surface current and electric field distributions. (a) Surface current distribution at 922 MHz. (b) Electric field distribution at 922 MHz.

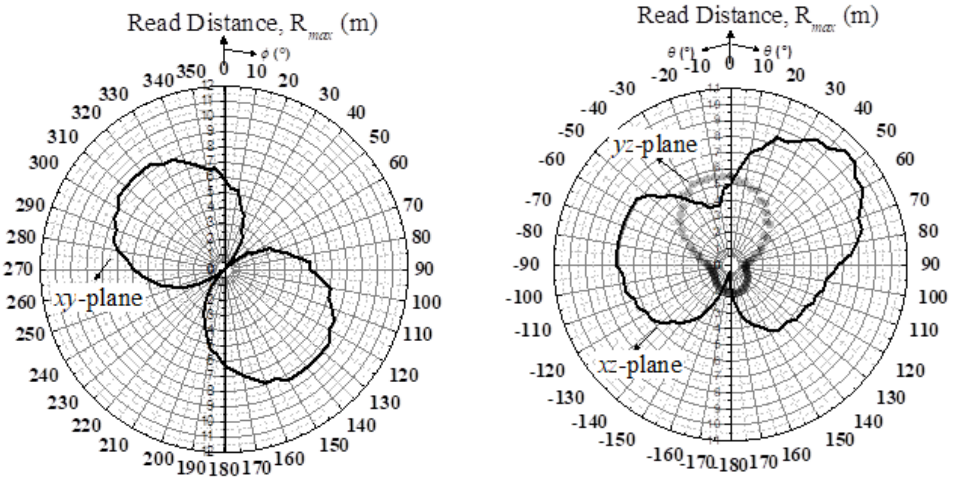

(a) (b)

Figure 7. Read patterns measured at 912 MHz. (a) Measured read pattern in the xy plane. (b) Measured read distance in the xz and yz planes.

stub located at the top-right corner as it functions as a shorting stub as well. Narrower and longer slots channel the currents to route a longer electrical path, and hence the tag resonant frequency shifts lower, miniaturizing the tag size.

It shows that the two C-shaped slots and thin inductive stubs in combination can be used for tuning the tag resonant frequency effectively. The slots are important as they can be used as an impromptu tuning mechanism. The corresponding electric field distribution is also shown in Fig. 6(b). The electric fields are observed to have a higher intensity around the microchip. The fields weaken near the inductive stub, which is shorting the radiating patch to the ground plane.

Figure 7(a) shows the measured read pattern in the xy plane at 912 MHz. A maximum read distance of ~ 8 m is observed in the directions of $\phi = 135°$ and $315°$. Fig. 7(b) shows the read distances in the xz and yz planes at the resonance. The read distance is found to be 5.5 m when the proposed tag is aligned in parallel with the reader antenna ($\theta = 0°$). No signal is detected in the reverse side due to the existence of the backing copper plate. Detailed description on the measurement processes can also be found in [6].

To study the effects of the backing metal plate, the tag antenna is positioned at the center of a copper plate with different sizes, and the corresponding read distances are all measured in the direction ($\theta = 45°$ and $\phi = 0°$). Fig. 8 shows the measured results for different plate lengths (L) and plate widths (W). In general, best read range is found to be in the range of 910–915 MHz. With reference

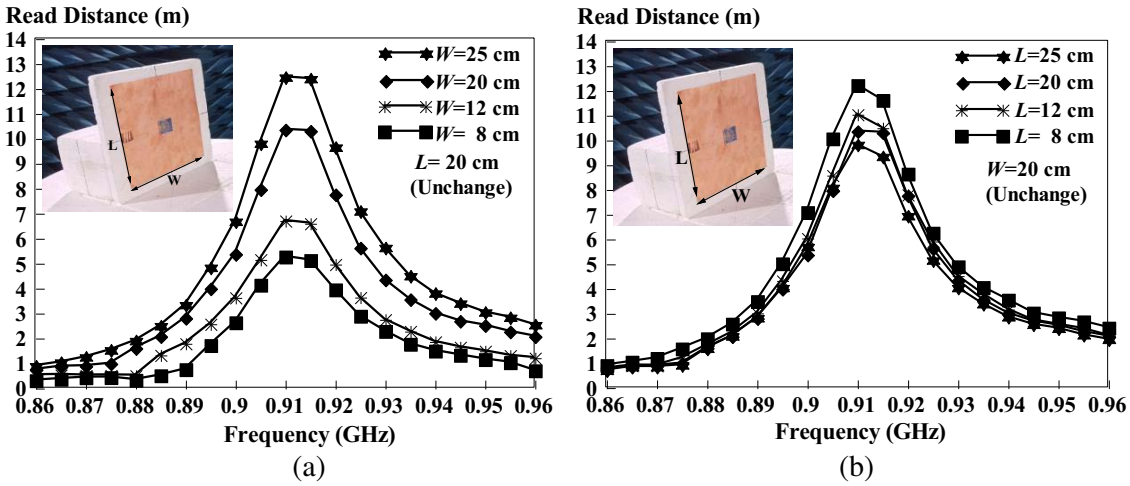

Figure 8. Measured read distances for copper plates with different sizes. (a) Varying W. (b) Varying L.

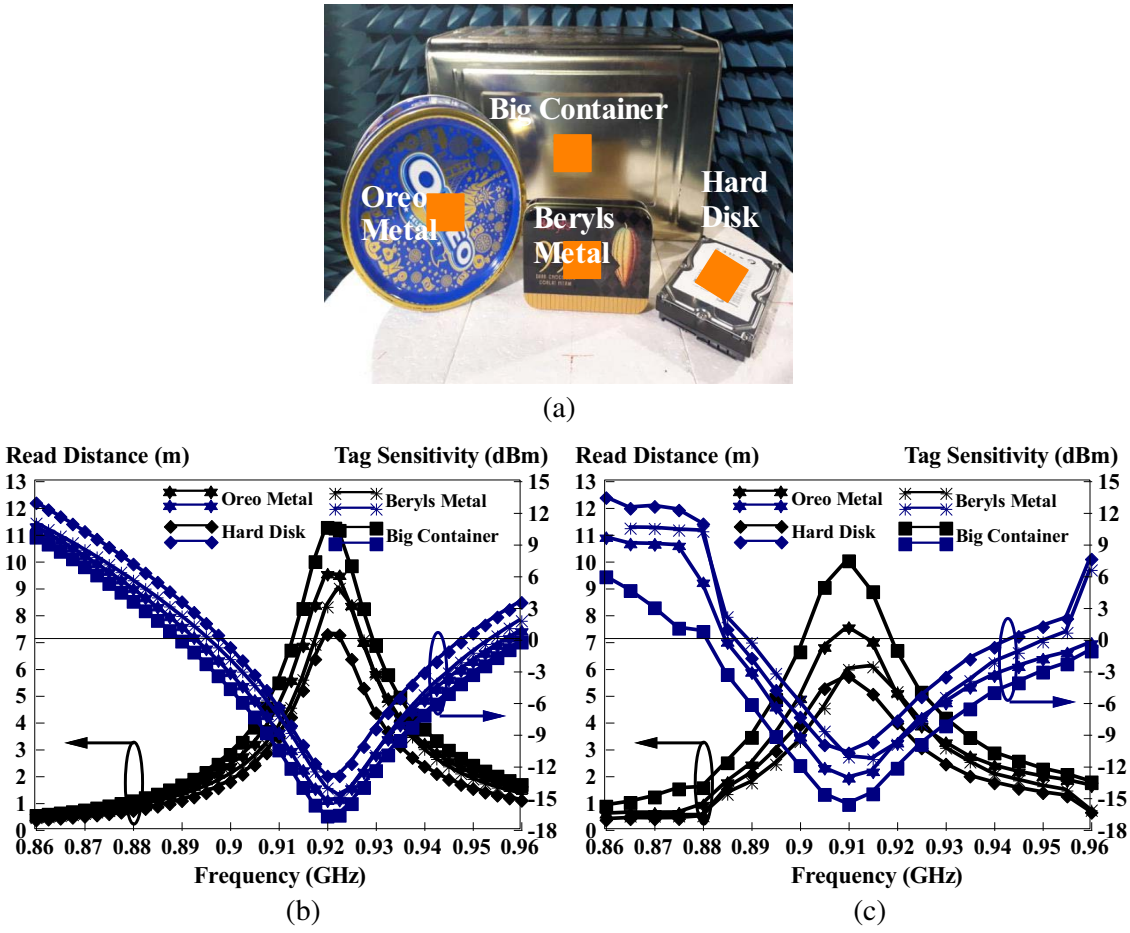

Figure 9. (a) Metallic objects, (b) simulated read distances and tag sensitivities and (c) measured read distances and tag sensitivities when the proposed tag is tested using the metallic objects at the direction of $\theta = 45°$ and $\phi = 0°$.

to Fig. 8(a), it can be seen that when W is reduced from 25 cm to 8 cm, the read distance decreases substantially from 12 m to $\sim$ 5 m. It can also be seen from Fig. 8(b) that the read distance fluctuates in the range of 10–12 m when L is reduced from 25 cm to 8 cm.

The proposed tag antenna is also tested on several actual implementation scenarios. First, the read distances and tag sensitivities are measured by fixing the proposed tag antenna on four metallic

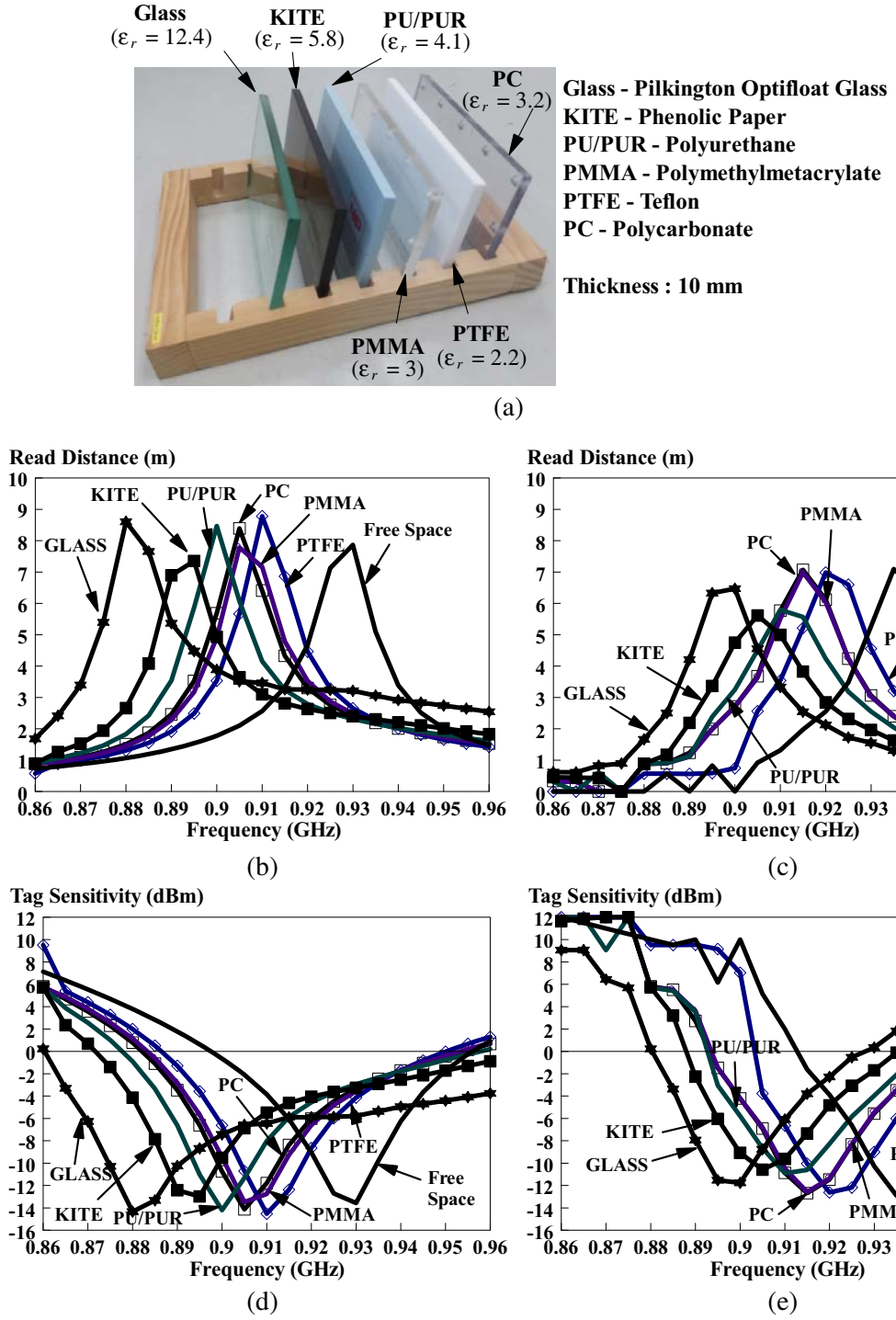

Figure 10. (a) NXP reference materials, (b) simulated read distances, (c) measured read distances, (d) simulated tag sensitivities and (e) measured tag sensitivities when the proposed tag is tested using the NXP reference materials at the direction of $\theta = 90^\circ$ and $\phi = 0^\circ$.

containers with different curvatures and sizes [shown in Fig. 9(a)]. With reference to the simulated results in Fig. 9(b), it is observed that the hard disk has the lowest read distance as it has the smallest surface area. The result matches well with the lowest tag sensitivity obtained in the same measurement. On the other hand, the proposed tag can be read from a farther distance, with a better tag sensitivity when it is placed on a bigger metallic container. Since the metallic containers in Fig. 9(a) were grocery items randomly purchased from a department store, their materials, coatings, compositions, and exact curvatures were actually not known. We could only estimate the shapes and simulate them as generic metallic objects. It has caused the measurement results to be slightly different from their simulation counterparts. In spite of the differences, their changing trends agree quite well. It is shown that the simulation model is able to forecast the measurement results reasonably well.

Although the tag antenna is designed for on-metal applications, its performance on non-conductive materials is worth knowing. The NXP reference materials [14] (24 cm × 12 cm × 1 cm), as shown in Fig. 10(a), are used for this evaluation. Figs. 10(b) and 10(c) are the simulated and measured read distances, respectively. Figs. 10(d) and 10(e) show the tag sensitivities. It can be seen that when a tag antenna is placed on a backing object with high dielectric constant, the resonant frequency will get detuned due to the dielectric loading effect. The resonance frequency shifts lower as the dielectric constant increases. A maximum read distance of greater than 5.5 m is observed for all cases. Despite the slight discrepancies, which are caused by tag fabrication and chip tolerances, the simulation models are able to predict the measurement results quite well.

In Table 2, the performance of the proposed tag antenna is compared with some of the contemporary metal-mountable UHF RFID tags. To minimize the tag antenna footprint, ceramic substrates with a higher relative permittivity such as Barium Titanate (BaTiO3) is used for designing a compact tag, with the price of higher costs [15]. In [6], the folded-patch structure is used to design metal-mountable tags, but due to the low antenna resistance, their power transmission coefficients are very low. Both tags in [16] and [20] use shorting vias in their designs, which will significantly increase the manufacturing costs and structural complexity. Good-performance miniaturized tags can be found in [17] and [18], but both involve a higher fabrication cost due to their double folding processes. Although the RFID tag in [19] can provide a longer reading distance, it is too large to be suitable for most of the practical applications. In contrast, our proposed tag has a compact footprint, achieving a good 10 m detectable range, which is suitable for applications that require long read ranges. Most importantly, it can be mounted on an

Table 2. Comparison of metal-mountable UHF RFID tag antennas.

Ref.	Power	Substrate Material	Tag/Antenna Structure	Flexibility	Manufacturing Complexity	Tag Volume (mm^3)	Backing Plate Size (cm)	Chip's Read Sensitivty (dBm)	Realized Gain (dBi)	Max. Read Distance (m)	Norm. Read Distance (m)
This work	4 W	Soft Polyethylene Foam	Folded-patch Antenna	Yes (soft foam)	simple	30 × 30 ×3 = 2700	20 × 20	−20	−4.35	10	10
[15]	4 W	Ceramic Substrate (Barium Titanate)	Slot Antenna	No (FR4 & ceramic)	simple (single folded)	594 × 2.91 = 1729	20 × 20	−18	−13.25	2.85	3.59
[6]	3.28 W	Soft Polyethylene Foam	Folded-patch Antenna	Yes (soft foam)	moderate (double folded)	40 × 40 ×1.6 = 2560	20 × 20	−20	−10.37	5	5.55
[16]	3.28 W	FR4	Inverted-F Antenna	No (FR4)	high (involved vias)	100 × 35 ×3 = 10500	21 × 13	−18	−6.5	6.2	8.67
[17]	4 W	Soft Polyethylene Foam	Folded-patch Antenna	Yes (soft foam)	moderate (double folded)	30 × 25 ×3 = 2250	20 × 20	−20	−5.36	8.9	8.9
[18]	4 W	Soft Polyethylene Foam	Dipolar Patch Antenna	Yes (soft foam)	moderate (double folded)	20 × 18 ×1.7 = 612	20 × 20	−17.8	−5.89	6.5	8.37
[19]	4 W	Soft Polyethylene Foam	Patch Antenna	No (soft foam with metal plate)	high (extra feeding part inserted in the middle of two patches)	72.1 × 25.5 ×3.2 = 5883	20 × 20	−14	0.64	8.9	17.76
[20]	4 W	FR4	Dual-layer Antenna with Parasitic Patch	No	high (two layer antenna with vias)	28 × 14 ×3.2 = 1254	20 × 20	−15	−14.24	1.8	3.2

*Normalized read distance, Power = 4 W, Chip Sensitivity = −20 dBm.

object with any size or shape. To improve the tuning flexibility of the operating frequency, our proposed tag has incorporated two large C-shaped slots for on-the-fly tuning without deteriorating the maximum read distance.

4. CONCLUSIONS

A compact folded-patch antenna, which has two large C-shaped slots for tuning its tag resonant frequency on the fly, has been proposed for designing a metal-mountable tag. The slots have functioned well as an impromptu tuning mechanism, and they are large enough to be modifiable by a penknife and some copper tapes. Having an impromptu tuning mechanism is useful for correcting those deviated tags in the production lines. It has been found that the two slots can tune the tag resonance effectively and arbitrarily to shift the deviated frequency back to the targeted value. The slots are tactfully embedded into the patch itself so that it virtually occupies no footprint. Measurements show that the proposed tag antenna is able to achieve a far read distance of more than 10 m on metal and greater than 5.5 m on dielectrics.

REFERENCES

1. UHF RFID Tags, "Smart retail solution," http://www.thinkgo.co/pinguan-iot-technology-co-ltd-rfid-label-15833051498388722.html.
2. Dobkin, D. M. and S. M. Weigand, "Environmental effects on RFID tag antennas," *IEEE MIT-S Int. Microw. Symp. Dig.*, 135–138, Jun. 2005, doi: 10.1109/MWSYM.2005.1516541.
3. Park, I. Y. and D. Kim, "Artificial magnetic conductor loaded long-range passive RFID tag antenna mountable on metallic objects," *Electron. Lett.*, Vol. 50, No. 5, 335–336, Feb. 2014, doi: 10.1049/el.2013.2671.
4. Babar, A. A., T. Björninen, V. A. Bhagavati, L. Sydänheimo, P. Kallio, and L. Ukkonen, "Small and flexible metal mountable passive UHF RFID tag on high-dielectric polymer-ceramic composite substrate," *IEEE Antennas Wave Propag. Lett.*, Vol. 11, 1319–1322, 2012, doi: 10.1109/LAWP.2012.2227291.
5. Bong, F. L., E. H. Lim, and F. L. Lo, "Flexible folded-patch antenna with serrated edges for metal-mountable UHF RFID tag," *IEEE Trans. Antennas Propag.*, Vol. 65, No. 2, 873–877, Feb. 2017, doi: 10.1109/TAP.2016.2633903.
6. Ng, W. H., E. H. Lim, F. L. Bong, and B. K. Chung, "Folded dipolar patch antenna with tunable inductive slots and stubs for UHF tag design," *IEEE Trans. Antennas Propag.*, Vol. 66, No. 6, 2799–2806, Jun. 2018, doi: 10.1109/TAP.2018.2821702.
7. ECCOSTOCK PP, accessed on Dec. 14, 2011. [Online]. Available: http://www.eccosorb.com/Collateral/Documents/English-US/PP.pdf.
8. Bong, F. L., E. H. Lim, and F. L. Lo, "Compact folded dipole with embedded matching loop for universal tag applications," *IEEE Trans. Antennas Propag.*, Vol. 65, No. 5, 2173–2181, May 2017, doi: 10.1109/TAP.2017.2676776.
9. Monza R6 Tag Chip Datasheet, Rev 3, document IPJ-W1700, Impinj, Inc., Seattle, WA, USA, Dec. 2014.
10. Manzari, S., S. Pettinari, and G. Marrocco, "Miniaturised wearable UHF-RFID tag with tuning capability," *Electron. Lett.*, Vol. 48, No. 21, 1325–1326, Oct. 2012, doi: 10.1049/el.2012.2813.
11. VoyanticTagformance Lite. [Online]. Available: https://voyantic.com/products/tagformance-lite.
12. Lee, Y. H., E. H. Lim, F. L. Bong, and B. K. Chung, "Folded antipodal dipole for metal-mountable UHF tag design," *IEEE Trans. Antennas Propag.*, Vol. 66, No. 11, 5698–5705, Nov. 2018.
13. Silva, S. B. and A. R. Correia, "Minimum activation power of a passive UHF RFID tags: A low cost method," *J. Aerosp. Technol. Manag.*, Vol. 10, e2418, doi: 10.5028/jatm.v10.854.
14. http://www.nxp.com/documents/application_note/AN162910.pdf.

15. Björninen, T., A. A. Babar, L. Ukkonen, L. Sydanheimo, A. Elsherbeni, and J. Kallioinen, "Compact metal mountable UHF RFID tag on a Barium Titanate based substrate," *Progress In Electromagnetics Research C*, Vol. 26, 43–57, 2012.
16. Tao, B., H. Sun, and O. M. Ramahi, "RFID tag antenna for metallic or non-metallic surfaces," *Progress In Electromagnetics Research C*, Vol. 59, 51–57, 2015.
17. Lee, S. R., E. H. Lim, F. L. Bong, and B. K. Chung, "Miniature folded patch with differential coplanar feedline for metal mountable UHF RFID tag," *IEEE J. RFID*, Vol. 68, No. 1, 152–160, Jan. 2020.
18. Niew, Y. H., K. Y. Lee, E. H., F. L. Bong, and B. K. Chung, "Miniature dipolar patch antenna with nonresonating ring for metal-insensitive UHF RFID tag design," *IEEE Trans. Antennas Propag.*, Vol. 68, No. 3, 2393–2398, Mar. 2020.
19. Son, H. W. and S. H. Jeong, "Wideband RFID tag antenna for metallic surfaces using proximity-coupled feed," *IEEE Antennas Wireless Propag. Lett.*, Vol. 10, 377–380, 2011.
20. Zhang, J. and Y. Long, "A miniaturized via-patch loaded dual-layer RFID tag antenna for metallic object applications," *IEEE Antennas Wireless Propag. Lett.*, Vol. 12, 1184–1187, 2013.